Published on 06 January 2009. Downloaded by Pohang University of Science and Technology on 30/05/2015 15:10:45.

Journal of Materials Chemistry

www.rsc.org/materials

Volume 19 | Number 7 | 21 February 2009 | Pages 809–1044

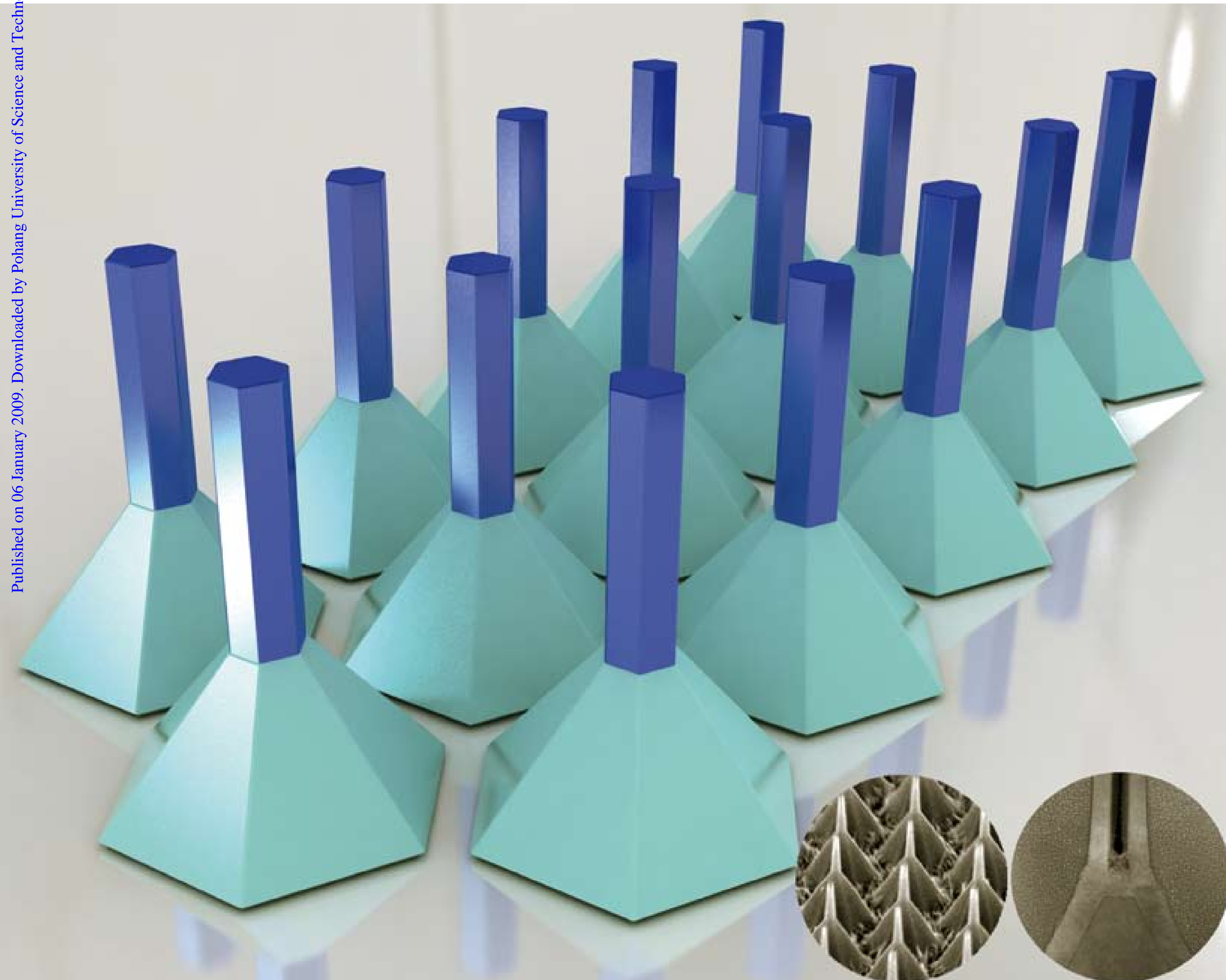

Inorganic nanotubes and nanowires

ISSN 0959-9428

PAPER
Gyu-Chul Yi *et al.*
Controlled epitaxial growth modes of ZnO nanostructures using different substrate crystal planes

FEATURE ARTICLE
Dmitri Goldberg *et al.*
Properties and engineering of individual inorganic nanotubes in a transmission electron microscope

RSC Publishing

Controlled epitaxial growth modes of ZnO nanostructures using different substrate crystal planes†

Young Joon Hong,[a] Jinkyoung Yoo,[a] Yong-Joo Doh,[a] Suk Hoon Kang,[b] Ki-jeong Kong,[c] Miyoung Kim,[b] Dong Ryeol Lee,[d] Kyu Hwan Oh[b] and Gyu-Chul Yi‡*[a]

Received 16th September 2008, Accepted 6th November 2008
First published as an Advance Article on the web 6th January 2009
DOI: 10.1039/b816034a

Published on 06 January 2009. Downloaded by Pohang University of Science and Technology on 30/05/2015 15:10:45.

A combined experimental and theoretical investigation has clarified the nanometre-scale vapour-phase epitaxial growth of ZnO nanostructures on different crystal planes of GaN substrates. Under typical growth conditions, ZnO nanorods grow perpendicular to the GaN(0001) plane, but thin flat films form on GaN(10$\bar{1}$1), (10$\bar{1}$0) and (11$\bar{2}$0). High-resolution X-ray diffraction data and transmission electron microscopy confirm the heteroepitaxial relationship between the ZnO nanostructures and GaN substrates. These results are consistent with first-principles theoretical calculations, indicating that the ZnO surface morphologies are mainly influenced by highly anisotropic GaN/ZnO interface energies. As a result of the large surface energy gradients, different ZnO nanostructures grow by preferential heteroepitaxial growth on different facets of regular GaN micropattern arrays. High-resolution transmission electron microscopy shows that ZnO nanotubes develop epitaxially on micropyramid tips, presumably as a result of enhanced nucleation and growth about the edges.

1. Introduction

Only in recent years has much attention been paid to bottom-up fabrication of one-dimensional (1D) crystalline semiconductor nanostructures, such as those used in nanometre-scale electronic and photonic devices.[1] In contrast, conventional thin film growth employed in top-down device production has been a major research field for several decades. In high-quality epitaxial thin film growth, it is imperative that consideration is given to strains induced by mismatches in lattice constants, thermal expansion coefficients, or both.[2] However, such strains can be significantly reduced through nanometre-scale epitaxy (nanoepitaxy) of 1D nanostructures. For example, vertically well-aligned 1D ZnO and GaN single crystalline nanorods grown on a Si substrate by nanoepitaxy do not show any significant structural defects, including dislocations.[3–5] On the other hand, the corresponding epitaxial thin films show sizeable dislocation and crack densities. Furthermore, position-controlled nanoepitaxy would be well suited for production of 1D nanostructures for three-dimensional integration of nanodevices. The use of controlled nanoepitaxy necessarily requires an understanding of those factors critical to growth of either two-dimensional thin films or 1D nanostructures. The present report concerns a combined experimental and theoretical investigation of catalyst-free, metal–organic vapour-phase epitaxy (MOVPE) of ZnO on various GaN substrate planes. The results demonstrate that the surface morphologies of the resulting ZnO nanostructures are governed by the highly anisotropic surface energies of the substrate.

Both single crystalline Al_2O_3 and GaN substrates have been widely used to yield high-quality epitaxial growth of both ZnO thin films[6,7] and nanorods.[3,8,9] Both substrates exhibit only a small lattice mismatch with, and have a similar crystal structure to, ZnO. However, it has not been established which parameters or mechanisms produce thin films and which yield nanorods during heteroepitaxy. In particular, most growth-mode control of ZnO has involved varying kinetic growth parameters, such as temperature and pressure, that affect surface diffusion of the adatoms.[10] Few studies have been undertaken of the effect of substrate orientation or well-faceted micropatterns on the growth mode. Both Al_2O_3 and GaN substrates possess highly anisotropic surface energies due to their anisotropic crystal structures ($a = b = 4.785$ and $c = 12.991$ Å for corundum Al_2O_3, and $a = b = 3.186$ and $c = 5.178$ Å for wurtzite GaN). As a result, different epitaxial growth modes of ZnO are expected on different substrate crystal planes. In this report, we demonstrate that the crystal orientation of the substrate is one of the main factors determining the surface morphologies of the nanostructures.

2. Experimental

ZnO nanostructures were grown using a low-pressure, catalyst-free MOVPE method. Diethylzinc (DEZn) and oxygen were employed as reactants and argon was used as a carrier gas. The flow rates of DEZn and oxygen were 3.0 and 20 standard cubic centimetres per minute (sccm), respectively. During growth,

[a]National Creative Research Initiative Center for Semiconductor Nanorods and Department of Materials Science and Engineering, POSTECH, Pohang, Gyeongbuk, 790-784, Korea. E-mail: gyuchul.yi@gmail.com
[b]Department of Materials Science and Engineering, Seoul National University, San 56-1, Seoul, 151-744, Korea
[c]Korea Research Institute of Chemical Technology, P. O. Box 107, Yuseong, Daejeon, 305-600, Korea
[d]Department of Physics, Soongsil University, Seoul, 156-743, Korea
† This paper is part of a *Journal of Materials Chemistry* theme issue on Nanotubes and Nanowires. Guest editor: Z. L. Wang.
‡ Present address: Department of Physics and Astronomy, Seoul National University, Seoul 151-747, Korea.

This journal is © The Royal Society of Chemistry 2009

Published on 06 January 2009. Downloaded by Pohang University of Science and Technology on 30/05/2015 15:10:45.

argon flowed into the quartz reactor through the bubbler with a DEZn bubbler temperature of −15 °C. To prevent premature reaction, the oxygen gas line was separated from the main gas manifold line. The reactor pressure and temperature were kept at 0.3 Torr and 500 °C. The GaN hexagonal micropatterns used for morphology-controlled selective growth of ZnO nanorods and nanotubes were prepared by conventional MOVPE and lithography techniques. The micropatterns were fabricated on Si(111) substrates using selective area MOVPE. A 1 μm thick GaN epitaxial seed layer with a 50 nm thick AlN buffer layer was by first deposited on Si(111), followed by a 50 nm thick SiO_2 layer using plasma-enhanced chemical vapour deposition. The SiO_2 layer was employed as a growth mask for the selective growth of the GaN micropattern arrays. Standard lithography and wet chemical etching were employed to develop submicron SiO_2 hole patterns on the GaN/Si(111) substrates. The GaN micropatterns were then selectively grown on the patterned substrates by MOVPE, with trimethylgallium (TMGa) and ammonia (NH_3) as reactants and purified hydrogen as the carrier. The NH_3 and TMGa flow rates were in the range of 10–50 sccm and 10–20 μmol min^{-1}, respectively. Si-striped micropatterns were formed by photolithography and KOH wet-chemical etching.

Morphological inspection and the structural analysis of the ZnO nanorods and nanotubes were undertaken with field-emission scanning electron microscopy (FE-SEM; Philips XL30SFEG) and high-resolution transmission electron microscopy (HR-TEM; FEI Tecnai F20). For TEM imaging and electron diffraction analysis, samples were milled with 30 kV-accelerated Ga ions using a focused ion beam machine (NOVA 200 Nanolab, FEI Company). The crystal structure and orientation of the samples were investigated by typical laboratory-radiation X-ray diffraction (XRD) setup or synchrotron-radiation X-ray diffraction (SR-XRD; 3C2 and 10C1 beamline at the Pohang Accelerator Laboratory).

The theoretical investigation of the interface formation energies and of the surface energies of the ZnO crystals on GaN was conducted by a series of first-principles calculations of the surface formation energies of ZnO crystals using the Vienna *ab initio* simulation program (VASP).[11] Calculations were carried out with ultrasoft pseudopotentials[12] by using plane waves up to a cut-off energy of 29.1 Ry (396 eV). For some calculations, the cut-off energy was increased to 33.0 Ry to check convergence of the results. The exchange-correlation potential was described within the generalized gradient approximation (GGA) parameterized by Perdew and Wang,[13] and Brillouin-zone integrals were determined through summations over sufficiently dense meshes of special points, at least 30 $\boldsymbol{k}$-points per 1 × 1 surface unit cell. All surfaces were represented by a periodically repeated symmetric slab consisting of several atomic layers, and were separated by a vacuum region with a thickness ranging from 12.9 to 15.3 Å. Slabs with 10–13 atomic layers (containing up to 60 atoms) were used for the (0001) and $\{11\bar{2}0\}$ surfaces, and 18–30 atomic layers (containing also up to 60 atoms) were used for the $\{10\bar{1}0\}$ and $\{10\bar{1}1\}$ surfaces. For polar (0001) surfaces, a dipole correction was used to prevent artificial electrostatic interactions between the repeated units. To simulate the underlying bulk structure, the slab lattice constant was set equal to the theoretical equilibrium bulk value in a direction parallel to the surface, and the atomic positions in two or three atomic layers in the centre of the slab were fixed at their bulk values.

3. Results and discussion

ZnO nanorods can be grown on many different substrates without using any metal catalysts, such as those that have been employed in catalyst-assisted growth. Fig. 1 displays FE-SEM images of ZnO nanorods grown on polycrystalline metal film, amorphous glass, Si(100), and Al_2O_3(0001) substrates by catalyst-free MOVPE under typical growth conditions. The results show clearly that vertical, well-aligned ZnO nanorods with similar diameters, 50 ± 5 nm, develop on all these substrates in similar numbers, ∼2 × 10^{10} cm^{-2}, even in the absence of any epitaxial relationship.

The crystallographic orientation and vertical alignment of the ZnO nanorods were investigated using X-ray diffractometry. Fig. 1(e) shows a θ-2θ scan of the nanorods in the 2θ range of 20–80°. Apart from the diffraction lines of the substrate, it shows 2θ peaks at only 34.43 and 72.60°, corresponding to (0002) and

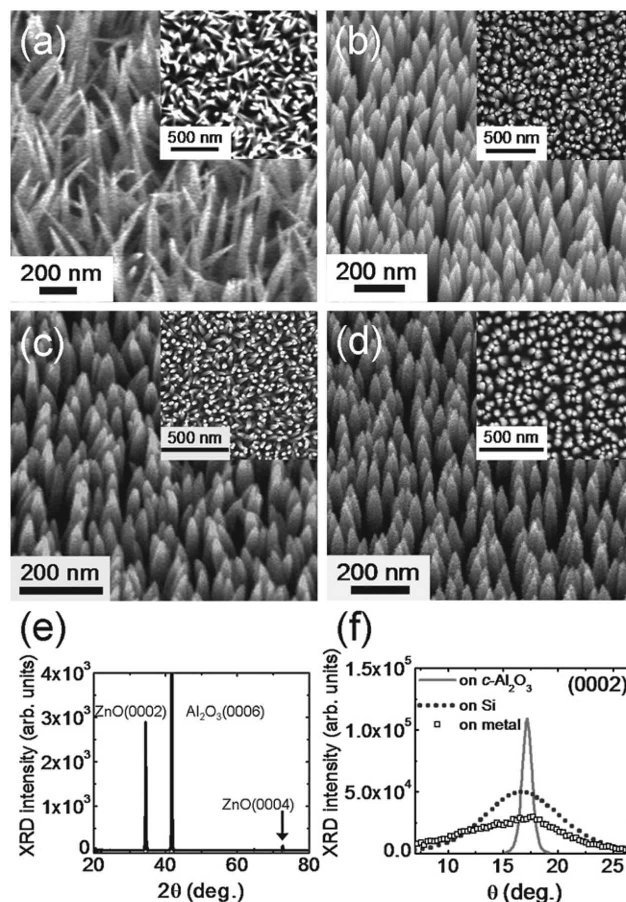

Fig. 1 FE-SEM images of ZnO nanorods grown on: (a) a platinum layer/Si substrate, (b) a glass substrate, (c) a Si(100) substrate, and (d) an Al_2O_3(0001) substrate. Insets correspond to top view of FE-SEM views. (e) XRD θ-2θ scan of vertically aligned ZnO nanorods. (f) θ-scan rocking curves around ZnO(0002) reflections obtained from ZnO nanorods grown on Pt/Si, Si, and Al_2O_3 substrates. FWHM values of θ-scan rocking curves were 1, 7, and 11° for *c*-Al_2O_3, Si, and metal substrates, respectively.

 This journal is © The Royal Society of Chemistry 2009

Published on 06 January 2009. Downloaded by Pohang University of Science and Technology on 30/05/2015 15:10:45.

(0004) planes of ZnO, respectively. All other samples in Fig. 1(a)–(d) showed similar XRD patterns, indicating that the ZnO nanorods were oriented with their *c*-axes along their hexagonal prismatic axes. This vertical alignment of the ZnO nanorods was confirmed by θ-scan rocking curves of XRD about the (0002) diffraction line of ZnO. Full width at half maximum (FWHM) values of the θ-scan rocking curves were 1, 7, and 11° for the *c*-Al_2O_3, single crystalline Si with a native oxide layer, and polycrystalline metal substrates, respectively. From both SEM inspection and XRD analyses, it is evident that the surface morphology of ZnO grown on all substrates is dominated by a coincidence of vertical prismatic growth with their *c*-axis and the vertical alignment of the ZnO nanorods is enhanced when the epitaxial relationship exists with the substrate.

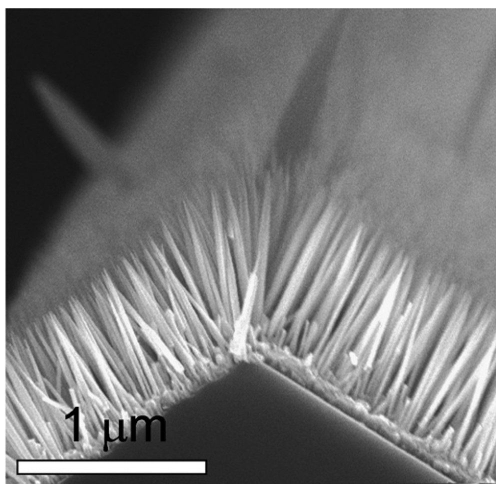

Fig. 2 Cross-sectional FE-SEM image of ZnO nanorods grown on Si micropatterns with Si{111} facets at the side and Si(100) as the basal plane.

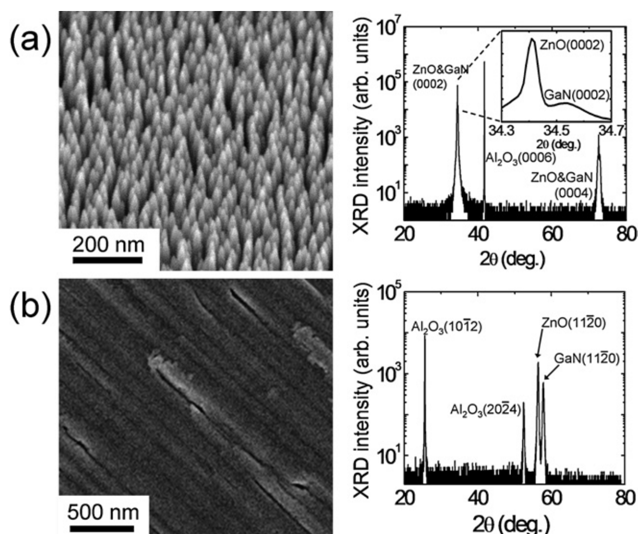

Fig. 3 FE-SEM bird's-eye images of ZnO: (a) vertical nanorods grown on GaN(0001)/Al_2O_3(0001) and (b) a thin film on GaN(11$\bar{2}$0)/Al_2O_3(10$\bar{1}$2) substrates. Each GaN layer was coated epitaxially on Al_2O_3 substrates with different crystal orientations. Corresponding XRD scan data depict the clear epitaxial relationship between ZnO and GaN.

Similar growth behaviour occurred even with patterned amorphous SiO_2/Si substrates, which lack any epitaxial relationship with ZnO. As shown in Fig. 2, vertically aligned ZnO nanorods formed uniformly across the entire surface of patterned SiO_2/Si. It is quite remarkable that the nanorod growth direction is again along the *c*-axis and perpendicular to the substrate surface. From these observations, it is inferred that the highly anisotropic surface energy of ZnO plays a dominant role in determining nanorod growth.

When the substrates were replaced by GaN thin films with different crystal orientations, drastic changes occurred in the morphology of the ZnO crystals, as shown in Fig. 3. Epitaxial GaN thin films with (0001) and (11$\bar{2}$0) planes were prepared by conventional MOVPE methods using Al_2O_3(0001) and (10$\bar{1}$2) substrates, respectively, followed by immediate growth of ZnO on the GaN layers. The growth of ZnO on both the (0001) and (11$\bar{2}$0) GaN layers was performed simultaneously and under the same conditions as used for the ZnO nanorods in Fig. 1. FE-SEM imaging showed that a high density ($\sim 1.2 \times 10^{11}$ cm^{-2}) of ZnO nanorods formed perpendicular to GaN(0001), but a ZnO thin film developed on GaN(11$\bar{2}$0). An ω-2θ SR-XRD scan data in Fig. 3 showed the growth orientation was perpendicular to ZnO(0001) for the nanorods and perpendicular to ZnO(11$\bar{2}$0) for the thin film.

In contrast with previous results for ZnO nanorods grown on a variety of substrates which did not show any epitaxial relationship with ZnO, the surface morphology and population density of ZnO nanorods proved to be strongly affected by the crystal orientation of the epitaxial GaN substrate. A similar crystal-plane-dependent surface morphology occurred among ZnO nanorods grown on Al_2O_3(0001) and (10$\bar{1}$2) substrates (not shown here). These observations point to the substrate and its crystal orientation exerting a strong epitaxial constraint on the growth mode of the ZnO nanostructures.

This crystal plane-dependent epitaxial growth mode of ZnO was further explored using substrates consisting of GaN micropyramid arrays, as shown in Fig. 4. Each GaN micropyramid consists of a very sharp GaN(0001) tip with six inclined {10$\bar{1}$1} sidewalls. The FE-SEM image of Fig. 4(a) shows that a single ZnO nanorod grew on each GaN micropyramid tip. A magnified bird's-eye view in Fig. 4(b) shows each such ZnO nanorod is a hexagonal prism, and no other nanorods have developed upon the inclined micropyramid sidewalls. This result demonstrates that for a given set of growth conditions, ZnO nanorods grow preferentially on GaN(0001) rather than on {10$\bar{1}$1}.

A high-resolution SR-XRD ω-2θ scan of the ZnO nanorod arrays is shown in Fig. 5(a) for the range of 20–80°. It serves to confirm that growth of the nanorods has again occurred along their *c*-axis. The similar scan of Fig. 5(b) shows diffraction lines at 34.42, 34.58, and 35.6° resulting from *c*-plane (0002) reflections of the ZnO nanorods, GaN micropyramid, and AlN layers, respectively. The inset displays two distinct (0004) diffraction lines from the ZnO nanorods and the GaN micropyramid at $2\theta =$ 72.58 and 72.95°, respectively.

An *HL*-mesh contour map developed by reciprocal-space mapping (RSM) about the ZnO(0004) line is shown in Fig. 5(c). The diffraction lines of ZnO(0004) and GaN(0004) are located at the same H (= 0) value, demonstrating that the ZnO nanorod and the GaN pyramid possess identical *c*-axis crystallographic

Published on 06 January 2009. Downloaded by Pohang University of Science and Technology on 30/05/2015 15:10:45.

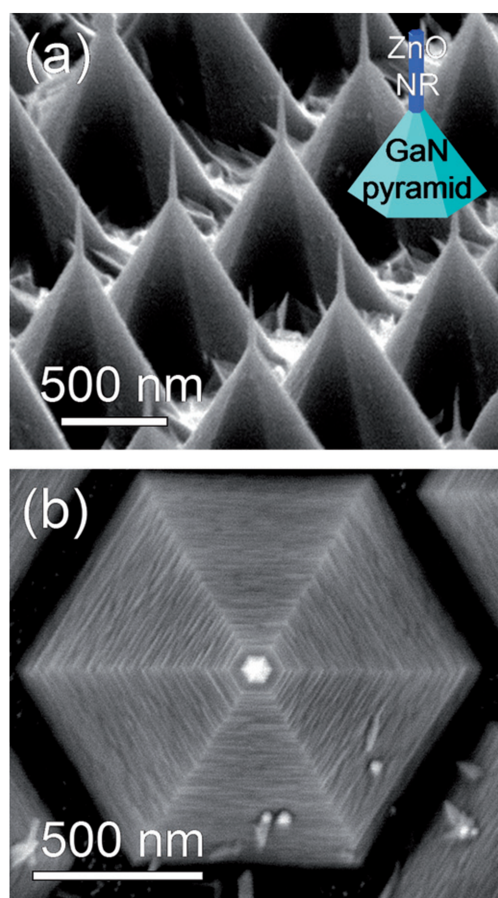

Fig. 4 FE-SEM images of site-selectively grown ZnO nanorods on top of hexagonal GaN micropyramid arrays in (a) bird's-eye and (b) top views. GaN micropyramid consists of a sharp tip of (0001) plane and six inclined sidewalls of $\{10\bar{1}1\}$ surfaces.

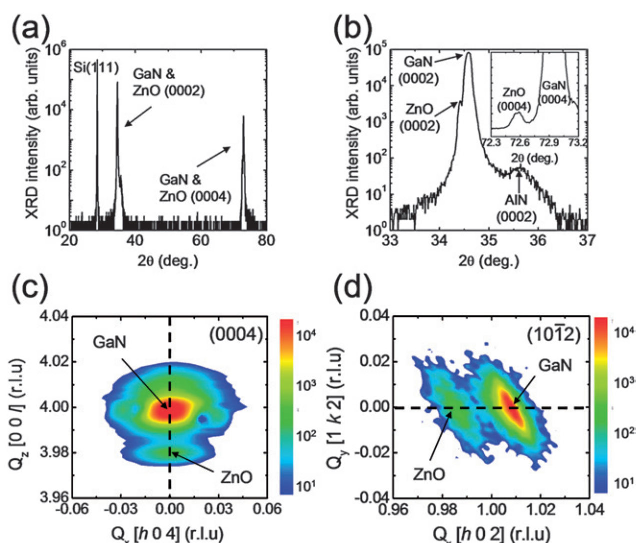

Fig. 5 High-resolution SR-XRD data of ZnO nanorods grown on GaN micropyramid arrays. (a) ω-2θ diffraction scan over the range of 20–80°. (b) Enlarged ω-2θ scan about ZnO(0002) and ZnO(0004) diffractions (inset). (c) *HL*-Mesh contour plot of the reciprocal-space map around (0004) diffractions of GaN and ZnO. (d) *HK*-mesh contour plot of the reciprocal-space map around $(10\bar{1}2)$ diffractions of GaN and ZnO. (The reciprocal lattice unit is abbreviated to r.l.u.; Q_x, Q_y, and Q_z correspond to *H*, *K*, and *L*, respectively.) The XRD data point to the ZnO nanorods growing heteroepitaxially on the GaN micropyramid patterns.

orientation. Furthermore, the diffraction trace along the dotted line in Fig. 5(c) shows distinct XRD lines at Q_z values of 3.98 and 4.00, corresponding to ZnO(0002) and GaN(0002), respectively. These results are consistent with the ZnO(0001) being congruent with GaN(0001) and with the *c*-axis of the nanorods being the same as their growth direction, normal to the substrate surface.

The in-plane epitaxial relationship between ZnO nanorods and GaN micropyramids on Si(111) was evaluated by measuring azimuthal (ϕ) scans of $\{10\bar{1}2\}$ diffractions and *HK*-mesh contour maps of RSM around $(10\bar{1}2)$ diffraction. The RSM contour map of Fig. 5(d) shows two well-resolved peaks corresponding to ZnO$(10\bar{1}2)$ and GaN$(10\bar{1}2)$, revealing a strong *in*-plane heteroepitaxial relationship between the ZnO nanorods and the GaN micropyramids. The contour map also shows that the diffraction peaks of ZnO$(10\bar{1}2)$ and GaN$(10\bar{1}2)$ lie along the same K (= 0) value, implying coherent epitaxial growth of ZnO nanorods with the GaN micropyramids. This observation confirms that the *c*-axis-oriented, single-crystal ZnO nanorods have grown heteroepitaxially on the GaN micropyramids, with a homogeneous and coherent *in*-plane alignment of ZnO nanorods.

The role of the substrate crystal plane in the selective formation of either a ZnO nanorod or a thin film was considered theoretically *via* a series of first-principles calculation using VASP.[11] For the calculations, ultra-soft pseudopotentials of plane waves and a cut-off energy of 29.1 Ry (396 eV) were employed. Details of the calculations are reported elsewhere.[14] Table 1 summarizes the calculation results of the surface formation energies of fundamental crystal planes of ZnO and GaN and the interface formation energies of a ZnO epitaxy on GaN.

Table 1 Theoretically calculated surface formation energies of GaN and ZnO crystals

Crystal planes	(0001)	$\{11\bar{2}0\}$	$\{10\bar{1}1\}$	$\{10\bar{1}0\}$
Surface formation energy of ZnO/J m^{-2}	1.91	1.02	1.57	1.01
Surface formation energy of GaN/J m^{-2}	2.64	1.53	1.76	1.40
Interface formation energy of ZnO on GaN/J m^{-2}	2.69	1.24	1.37	1.13

The typical growth behaviour of ZnO nanorods, as shown in Fig. 1, can be explained in terms of the highly anisotropic surface formation energies of ZnO.[15] Theoretical calculations show that the ZnO plane with the highest surface formation energy is (0001), and that the surface formation energy for the $\{10\bar{1}0\}$ plane is much smaller than for either $\{11\bar{2}0\}$ or (0001) planes. This implies that there would be a substantial energy gain in forming nanorods rather than a thin film upon reducing the surface area of ZnO(0001). A substrate with an isotropic surface energy will not provide any constraint towards 1D ZnO nanorod growth. ZnO nuclei can occur randomly across the entire substrate surface during initial growth, and subsequently transform into nanorods upon a reduction in the surface formation energy.

 This journal is © The Royal Society of Chemistry 2009

Published on 06 January 2009. Downloaded by Pohang University of Science and Technology on 30/05/2015 15:10:45.

For the heteroepitaxial growth of ZnO on GaN substrates, the interface formation energy needs to be considered in concert with the surface energy, given that the epitaxial relationship between ZnO and GaN strongly affects both the ZnO growth mode and morphology. At the GaN(0001) surface, the growth of ZnO nanorods with $\{10\bar{1}0\}$ sidewalls will be preferred in order to reduce the surface formation energy of ZnO(0001). This agrees with the experimental results shown in Fig. 3(a). For ZnO growth on the GaN$\{11\bar{2}0\}$ plane, however, the GaN$\{11\bar{2}0\}$ surface energy of 1.53 J m^{-2} is reduced to yield an interface formation energy of 1.24 J m^{-2} following initial deposition of the ZnO$(11\bar{2}0)$ film. An even smaller surface formation energy for the ZnO$(11\bar{2}0)$ plane of 1.02 J m^{-2} results in a ZnO film morphology rather than nanorods on the GaN$\{11\bar{2}0\}$ plane, as is consistent with our experimental observations shown in Fig. 3(b). The theoretical calculations also imply that GaN micropyramids with smooth sidewalls should be employed for the nanorod selective growth. If the surfaces of sidewalls have a combination of small (0001) ledges and $\{10\bar{1}0\}$ vertical walls, vertically aligned nanorods can be grown even on the sidewalls of GaN micropyramids.

Further, morphologically controlled growth of ZnO nanorods was obtained using a patterned array of GaN microrods, in which the topmost plane corresponded to GaN(0001) with six $\{10\bar{1}0\}$ sidewalls instead of $\{10\bar{1}1\}$. Fig. 6(a) and (b) show perpendicular ZnO nanorods have grown atop the (0001) GaN microrod surfaces only, consistent with both our previous observation in Fig. 4 and our theoretical calculations. However, SEM images clearly show that much higher density of ZnO nanorods has developed along the edges of the topmost hexagonal plane of each GaN microrod. These have even become interconnected at their bases, as shown in the enlarged view of Fig. 6. The ZnO nanorod density was estimated to be ~61 μm^{-1} along the edge lines and ~23 μm^{-1} inside the topmost plane, respectively. This result indicates that nucleation and growth activity was more intense among the ZnO nanorods about the periphery of the topmost GaN(0001) plane.

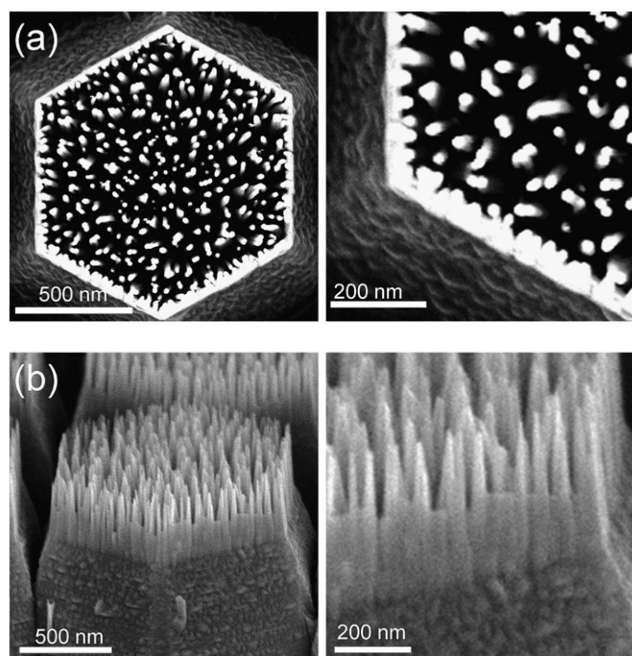

Fig. 6 FE-SEM images of ZnO nanorods atop the GaN microrod patterns in (a) top and (b) bird's-eye views, respectively. A high density of ZnO nanorods have grown around the boundary of the uppermost planes of the GaN microrods. Enlarged views depict that the densely grown ZnO nanorods are connected to each other at their bases.

In addition, the enhanced nucleation along the edge line of the GaN(0001) topmost plane makes it possible to grow ZnO nanotubes rather than nanorods at GaN micropyramid tips, depending on the plane area of the tips. As shown in Fig. 7(a) and (b), a single ZnO nanotube has grown at the tip of a micropyramid with an extended top planar area. Empirically, a topmost plane area of about ~50 × 50 nm^2 was favourable for nanotube growth, while a much smaller plane area was required for nanorods.

The enhanced growth of ZnO nanorods around the peripheries points to the presence of a pronounced thermodynamic driving force coupled with a highly anisotropic surface formation energy. A three-dimensional Ehrlich–Schwoebel energy barrier exists in a well-faceted mesa structure and is encountered by an adatom when it diffuses from the sidewalls onto the top of the structure.[16] As a consequence, it is known to be both thermodynamically favourable and kinetically faster for adatoms to climb atop the mesa through a facet-step joint along the periphery.[16–18] When the lateral dimension (L) of the topmost plane of the

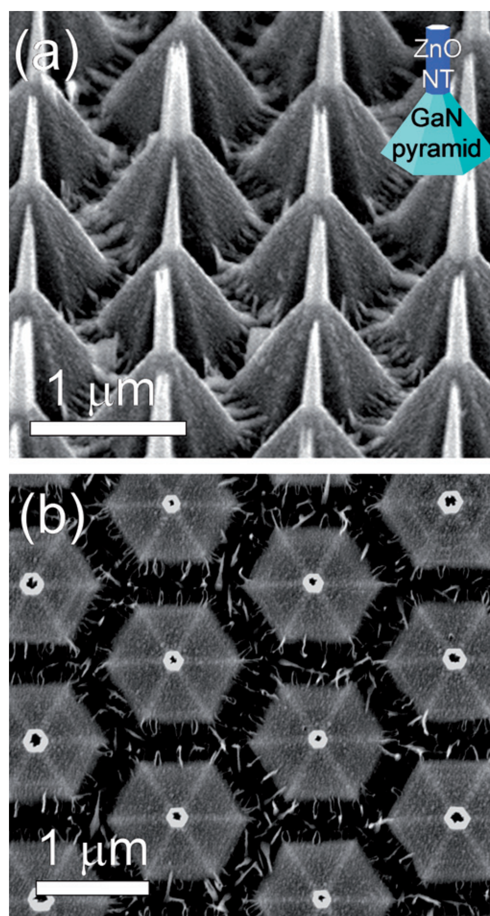

Fig. 7 Schematic and FE-SEM images of ZnO nanotubes atop the GaN micropyramid patterns in: (a) bird's-eye and (b) top views.

Published on 06 January 2009. Downloaded by Pohang University of Science and Technology on 30/05/2015 15:10:45.

micropyramid becomes small enough to be comparable with the surface diffusion length (λ_s),[19,20] multiple nuclei presumably residing on the edge line of the topmost plane can be connected with each other to form a single nanotube. In a limiting case of $L \ll \lambda_s$, however, a single nanorod is expected to form at the tip of the micropyramid as a result of a single nucleus, which is qualitatively in agreement with our observations.

The different morphologies of the ZnO nanostructures that develop on the GaN micropatterns of similar crystal orientation can be explained qualitatively by a surface diffusion process.[19,20] When the lateral dimension (L) of the topmost plane of the micropyramid is much larger than the surface diffusion length of an adatom, irregular nanorod arrays form inside the topmost plane with a high density of nanorods about the periphery, as observed in Fig. 6. As L becomes much smaller than the surface diffusion length, however, a single nanorod is expected to form from a single nucleus at the tip end of the micropyramid, as depicted in Fig. 4. When L becomes comparable with the surface diffusion length, multiple nuclei can reside on the edge line of the topmost plane and merge with each other to form a single nanotube, as shown in Fig. 7.

More precise information on the crystal structure and the relevant growth mode of ZnO is shown in a cross-sectional TEM image of a single ZnO nanotube grown atop a GaN micropyramid. Fig. 8(a) shows a thin, coexisting ZnO film has formed on the inclined $\{10\bar{1}1\}$ sidewalls of the GaN micropyramid, with an individual ZnO nanotube located at the GaN(0001) tip, consistent with previous theoretical calculations. The theoretical calculations also imply that GaN micropyramids with smooth sidewalls should be employed for the nanorod selective growth. If the surfaces of sidewalls have a combination of small (0001) ledges and $\{10\bar{1}0\}$ vertical walls, vertically aligned nanorods can be grown even on the sidewalls of GaN micropyramids. After one hour's growth, the length of the ZnO nanotube was ~950 nm, and the thickness of the ZnO thin film was ~50 nm. Fig. 8(b) shows a high-resolution TEM lattice image for the outlined area of Fig. 8(a), with arrows I_A and I_B indicating the interfaces between ZnO and GaN. The *c*-plane lattice slabs of GaN and ZnO are parallel with few discontinuities, showing that both the ZnO nanorod and the thin film have grown heteroepitaxially on the GaN micropatterns without the formation of any significant structural defects.

The above results offer a new approach for the selective growth of ZnO nanorods and nanotubes by utilizing micropatterned epitaxial GaN substrates. Preformed GaN micropyramids provide preferential growth sites. As a result of the strongly anisotropic surface and interface formation energies, ZnO nanorods and nanotubes develop at the GaN(0001) tips with none developing on the GaN$\{10\bar{1}1\}$ sidewalls. By utilizing such epitaxial growth modes and depending on the crystal orientation of the substrate, it becomes possible to design surface morphologies for individual nanostructures. This approach is distinct from other position-controlled growth techniques[21] that employ patterned metal catalysts[22–24] or catalyst-free amorphous growth masks.[25,26] Furthermore, when compared with other methods of fabricating inorganic nanotubes,[27] such as those that utilize selective etching of core materials in core–shell heterostructure nanowires[28] or interfacial solid-state diffusion between core–shell nanowires,[29] the epitaxial growth method

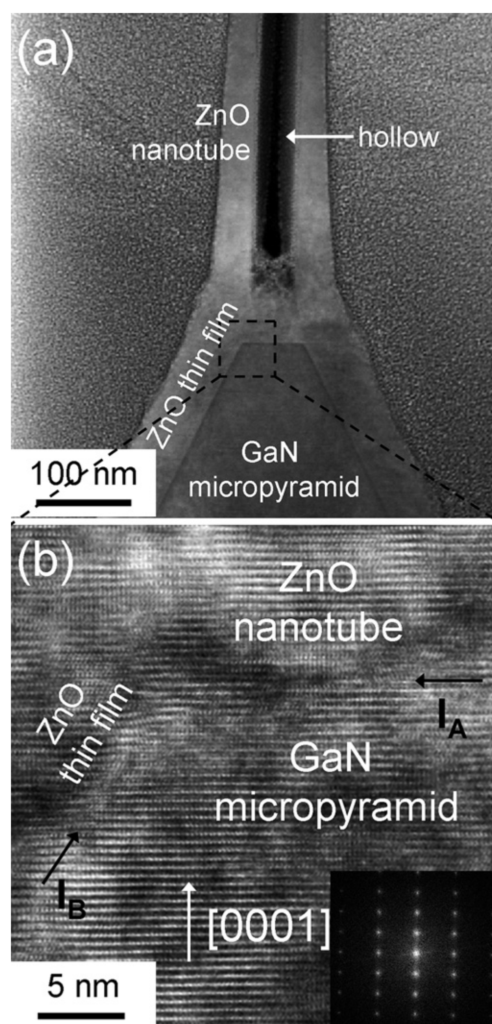

Fig. 8 (a) Cross-sectional annular dark field scanning transmission electron microscopy image of a single ZnO nanotube grown atop a GaN micropyramid. ZnO thin film formation has occurred on the sidewalls of GaN$\{10\bar{1}1\}$. (b) HR-TEM image of the selected area in (a) showing the epitaxial growth of the ZnO nanotube and thin film on the GaN micropyramid. The arrow I_A (I_B) shows the interface between the ZnO nanotube (thin film) and the topmost plane (sidewall) of the GaN micropyramid.

demonstrated here provides a rational route that avoids unintentional damage or contamination during etching or diffusion.

4. Conclusions

In summary, analysis of the surface morphologies and crystal structures of ZnO nanostructures produced by controlled heteroepitaxial growth on GaN substrates showed that spontaneous formation of either ZnO nanorods, nanotubes, or thin films strongly depends on the crystal plane of the GaN substrate, in contrast with the observation of the vertically aligned nanorod growths on the non-epitaxial substrates of glass, polycrystalline metal and silicon. The result is consistent with theoretical calculations of the anisotropic surface and interface formation energies. The large gradient in surface energies of GaN micropatterns allows us to control the surface morphology and growth

This journal is © The Royal Society of Chemistry 2009

Published on 06 January 2009. Downloaded by Pohang University of Science and Technology on 30/05/2015 15:10:45.

position concurrently during growth of ZnO nanorods and nanotubes. We believe that our experimental and theoretical investigations provide general knowledge for the catalyst-free selective formation of crystalline nanostructures with a desired morphology and arrangement. Furthermore, our investigation on the effect of surface and interface formation energies on nanoepitaxy of one-dimensional nanostructures may readily be expanded for position-controlled selective growth of many other semiconductor nanorods and nanotubes.

Acknowledgements

This work was financed by the National Creative Research Initiative Project (R16-2004-004-01001-0) of the Korea Science and Engineering Foundations (KOSEF). The work of Kim at Seoul National University was funded by grant No. R01-2006-000-11071-0 from the Basic Research Program of the Korea Science and Engineering Foundation. Kong at KRICT gratefully acknowledges support from the MOCIE of Korea through the National R&D Project for Nano Science and Technology. Experiments at Pohang Accelerator Laboratory (PAL) were funded in part by the Ministry of Science and Technology (MOST) and POSTECH.

References

1 C. M. Lieber and Z. L. Wang, *MRS Bull.*, 2007, **32**, 99.
2 M. A. Herman, W. Richter and H. Sitter, *Epitaxy: Physical principles and technical implementation*, Springer, Berlin, 2004.
3 W. I. Park, D. H. Kim, S.-W. Jung and G.-C. Yi, *Appl. Phys. Lett.*, 2002, **80**, 4232.
4 G.-C. Yi, C. Wang and W. I. Park, *Semicond. Sci. Technol.*, 2005, **20**, S22.
5 H.-M. Kim, D. S. Kim, Y. S. Park, D. Y. Kim, T. W. Kang and K. S. Chung, *Adv. Mater.*, 2002, **14**, 991.
6 X. W. Sun and H. S. Kwok, *J. Appl. Phys.*, 1999, **86**, 408.
7 S.-K. Hong, H.-J. Ko, Y. Chen, T. Hanada and T. Yao, *Appl. Surf. Sci.*, 2000, **159–160**, 441.
8 M. H. Huang, S. Mao, H. Feick, H. Q. Yan, Y. Wu, H. Kind, E. Weber, R. Russo and P. Yang, *Science*, 2001, **292**, 1897.
9 Y. W. Heo, D. P. Norton, L. C. Tien, Y. Kwon, B. S. Kang, F. Ren, S. J. Pearton and J. R. LaRoche, *Mater. Sci. Eng., R*, 2004, **47**, 1.
10 Z. L. Wang, *J. Phys.: Condens. Matter.*, 2004, **16**, R829.
11 G. Kresse and J. Hafner, *Phys. Rev. B*, 1993, **47**, 558.
12 D. Vanderbilt, *Phys. Rev. B*, 1990, **41**, 7892.
13 J. P. Perdew and Y. Wang, *Phys. Rev. B*, 1992, **45**, 13244.
14 T. W. Kim, Y. J. Hong, G.-C. Yi, J.-H. Kwon, M. Kim, H. N. Han, D. H. Kim, K. H. Oh, K.-J. Kong and Y.-K. Kwon, *J. Phys. D: Appl. Phys.*, 2008, **41**, 015406.
15 M. Kim, Y. J. Hong, J. Yoo, G.-C. Yi, G.-S. Park, K.-J. Kong and H. Chang, *Phys. Status Solidi RRL*, 2008, **2**, 197.
16 Y. Han, F. Liu, S.-C. Li, J.-F. Jia, Q.-K. Xue and B.-J. Lee, *Appl. Phys. Lett.*, 2008, **92**, 021909.
17 H. Okamoto, D. Chen and T. Yamada, *Phys. Rev. Lett.*, 2002, **89**, 256101.
18 C.-S. Jiang, S.-C. Li, H.-B. Yu, D. Eom, X.-D. Wang, P. Ebert, J.-F. Jia, Q.-K. Xue and C.-K. Shih, *Phys. Rev. Lett.*, 2004, **92**, 106104.
19 A. I. Persson, L. E. Froberg, S. Jeppesen, M. T. Björk and L. Samuelson, *J. Appl. Phys.*, 2007, **101**, 034313.
20 M. T. Borgström, G. Immink, B. Ketelaars, R. Algra and E. P. A. M. Bakkers, *Nat. Nanotechnol.*, 2007, **2**, 541.
21 H. J. Fan, P. Werner and M. Zacharias, *Small*, 2006, **2**, 700.
22 Y. Xia, P. Yang, Y. Sun, Y. Wu, B. Mayers, B. Gates, Y. Yin, F. Kim and H. Yan, *Adv. Mater.*, 2003, **15**, 353.
23 L. Samuelson, C. Thelander, M. T. Björk, M. Borgström, K. Deppert, K. A. Dick, A. E. Hansen, T. Mårtensson, N. Panev, A. I. Persson, W. Seifert, N. Sköld, M. W. Larsson and L. R. Wallenberg, *Physica E*, 2004, **25**, 313.
24 Y. W. Heo, V. Varadarajan, M. Kaufman, K. Kim, D. P. Norton, F. Ren and P. H. Fleming, *Appl. Phys. Lett.*, 2002, **81**, 3046.
25 J. Noborisaka, J. Motohisa and T. Fukui, *Appl. Phys. Lett.*, 2005, **86**, 213102.
26 S. D. Hersee, X. Sun and X. Wang, *Nano Lett.*, 2006, **6**, 1808.
27 M. Law, J. Goldberger and P. Yang, *Annu. Rev. Mater. Res.*, 2004, **34**, 83.
28 J. Noborisaka, J. Motohisa, S. Hara and T. Fukui, *Appl. Phys. Lett.*, 2005, **87**, 93109.
29 H. J. Fan, M. Knez, R. Scholz, K. Nielsch, E. Pippel, D. Hesse, M. Zacharias and U. Gösele, *Nat. Mater.*, 2006, **5**, 627.